1-1-2015

The Effects of Extending the Spectral Information Acquired by a Photon-counting Detector for Spectral CT

Taly Gilat Schmidt
Marquette University, tal.gilat-schmidt@marquette.edu

Kevin C. Zimmerman
kevin.zimmerman@marquette.edu

Emil Y. Sidky
University of Chicago

Accepted version. *Physics in Medicine and Biology*, Vol. 60, No. 4 (January 2015): 1583-1600. DOI.

The Effects of Extending the Spectral Information Acquired by A Photon-Counting Detector for Spectral CT

Taly Gilat Schmidt
Department of Biomedical Engineering, Marquette University, Milwaukee, WI
Kevin C. Zimmerman
Department of Biomedical Engineering, Marquette University, Milwaukee, WI
Emil Y. Sidky
Department of Radiology, University of Chicago, Chicago, IL

Abstract: Photon-counting x-ray detectors with pulse-height analysis provide spectral information that may improve material decomposition and contrast-to-noise ratio (CNR) in CT images. The number of energy measurements that can be acquired simultaneously on a detector pixel is equal to the number of comparator channels. Some spectral CT designs have a limited number of comparator channels, due to the complexity of readout electronics. The spectral information could be extended by changing the comparator threshold

Physics in Medicine and Biology, Vol 60, No. 4 (February 2015): pg. 1583-1600. DOI.

levels over time, sub pixels, or view angle. However, acquiring more energy measurements than comparator channels increases the noise and/or dose, due to differences in noise correlations across energy measurements and decreased dose utilisation. This study experimentally quantified the effects of acquiring more energy measurements than comparator channels using a bench-top spectral CT system. An analytical and simulation study modeling an ideal detector investigated whether there was a net benefit for material decomposition or optimal energy weighting when acquiring more energy measurements than comparator channels. Experimental results demonstrated that in a two-threshold acquisition, acquiring the high-energy measurement independently from the low-energy measurement increased noise standard deviation in material-decomposition basis images by factors of 1.5–1.7 due to changes in covariance between energy measurements. CNR in energy-weighted images decreased by factors of 0.92–0.71. Noise standard deviation increased by an additional factor of $\sqrt{2}$ due to reduced dose utilisation. The results demonstrated no benefit for two-material decomposition noise or energy-weighted CNR when acquiring more energy measurements than comparator channels. Understanding the noise penalty of acquiring more energy measurements than comparator channels is important for designing spectral detectors and for designing experiments and interpreting data from prototype systems with a limited number of comparator channels.

1. Introduction

Spectral computed tomography (CT) systems that use photon-counting detectors with pulse-height analysis are being developed with the potential to improve material decomposition and contrast-to-noise ratio (CNR) compared to conventional CT imaging approaches (Shikhaliev *et al* 2005, Roessl and Proksa 2007, Schlomka *et al* 2008, Shikhaliev 2008, Taguchi and Iwanczyk 2013). Photon-counting spectral CT is performed with direct-conversion semiconductor detectors. When a photon is absorbed in an ideal detector, a pulse with voltage proportional to the deposited energy is created by the readout electronics. The readout electronics contain N channels, where each channel consists of a comparator circuit and a counter. The comparator for each channel can be set to a different threshold level. For each channel, the counter is incremented if the pulse voltage is greater than the comparator threshold. At the end of a readout period, the resulting measurement is the number of photons detected above the energy threshold for each channel, resulting in N spectral measurements.

Some spectral CT designs have a limited number of comparator channels, due to the complexity of readout electronics that acquire

Physics in Medicine and Biology, Vol 60, No. 4 (February 2015): pg. 1583-1600. DOI.

simultaneous energy measurements. Additional energy measurements could be acquired by changing the threshold levels over time, sub pixels, or view angle. By adding more spectral information, these methods could potentially improve material decomposition or energy-weighted images. However, acquiring more energy measurements than comparator channels is expected to incur penalties in noise and dose, which is the subject of this paper.

A previous study proposed a 'chess board' detector where comparator channels were distributed spatially over sub-pixels to increase the number of energy measurements at the expense of spatial resolution (Kappler *et al* 2013). This previous work discussed the noise effects of the chess-board pattern detector, but did not explicitly quantify these effects.

Acquiring more energy measurements than comparator channels is required when a detector with a limited number of comparator channels is used to simulate a detector with more channels, for example to investigate feasibility and potential benefits of a more complex detector design (Procz *et al* 2009). Understanding the noise effects of acquiring more energy measurements than comparator channels is important for designing experiments and analysing the data from a detector with a limited number of comparator channels.

The purpose of this study was to quantify the noise effects and potential benefits of acquiring more energy measurements than comparator channels. Section 2 presents the theoretical noise properties of spectral CT acquisition methods, followed by a description of the experimental study that quantified the noise effects for material decomposition and energy weighting applications. Section 2 also describes the study that investigated whether there was a net benefit when acquiring more energy measurements than comparator channels for an ideal detector.

Physics in Medicine and Biology, Vol 60, No. 4 (February 2015): pg. 1583-1600. DOI.

2. Materials and methods

2.1. Theoretical noise properties

We use the term 'one-sided' energy measurement to refer to the number of photons detected above a threshold, which is the output of a comparator channel. Energy-resolved information can be obtained by subtracting two one-sided energy measurements. In an ideal detector, the difference between a lower-threshold energy measurement and a higher-threshold energy measurement is the number of photons detected between the two energy thresholds, which we refer to as a 'two-sided' energy bin.

2.1.1. Correlated one-sided energy measurements.

Two-sided energy bins are usually derived from N positively correlated, one-sided energy measurements acquired from N comparator channels on the same pixel at the same time. The noise in the one-sided energy measurements is Poisson distributed. Positive noise correlations occur because the channels see the same spectrum noise realisation and detect the same photon noise for their overlapping energy ranges. Positive noise correlation across energy measurements was previously determined to reduce noise in material decomposition estimates (Roessl *et al* 2007). Because two channels count the same number of photons above the higher threshold, the noise from the higher energies is removed when the higher-energy measurement is subtracted from the lower-energy measurement to form a two-sided bin. The noise in the resulting two-sided energy bin depends only on the noise of the energies spanned by that bin and is Poisson distributed with mean and variance equal to $\bar{\lambda}_i$, as expressed in equation (1), where $S(E)$ is the x-ray beam spectrum and $\mu(x, y, E)$ is the spatial distribution of the energy-dependant linear attenuation coefficient of the object, which is integrated along ray path $\vec{t}$. The highest energy bin is bounded by the maximum energy in the spectrum. After subtraction, the measured counts in the two-sided energy bins are uncorrelated for an ideal detector.

Physics in Medicine and Biology, Vol 60, No. 4 (February 2015): pg. 1583-1600. DOI.

$$\bar{\lambda}_i = \int_{E_i}^{E_{i+1}} S(E)\, \mathrm{e}^{-\int \mu(x,y,E)\mathrm{d}\vec{l}}\, \mathrm{d}E \qquad (1)$$

2.1.2. Independent one-sided energy measurements.

When more energy measurements are acquired than comparator channels, the additional one-sided energy measurements are statistically independent from the previously acquired energy measurements. In this case, two, one-sided energy measurements count different numbers of photons above the higher threshold. Subtracting the higher energy measurement from the lower energy measurement adds noise from the higher energies to the resulting two-sided energy bin. The subtraction of two independent Poisson random variables is not Poisson distributed, but is described by the Skellam distribution (Yavuz and Fessler 1999). The number of counts detected in a two-sided energy bin created from two independent one-sided energy measurements has a mean of $\bar{\lambda}_i$ and variance equal to $\bar{r}_i + \bar{r}_{i+1}$, where $\bar{r}_i$ is the mean number of counts above the *i*th threshold, as expressed in equation (2), where $E_{\max}$ is the highest energy in the spectrum. The subtraction of independent Poisson random variables also occurs in PET imaging, when the detected counts are corrected by subtracting the number of random counts estimated by a delayed channel. Previous work in PET imaging demonstrated bias if the noise statistics after subtraction are not accurately modelled in estimation tasks (Yavuz and Fessler 1999).

$$\bar{r}_i = \int_{E_i}^{E_{\max}} S(E)\, \mathrm{e}^{-\int \mu(x,y,E)\mathrm{d}\vec{l}}\, \mathrm{d}E \qquad (2)$$

In addition to the noise penalty due to changing the correlation across energy measurements, acquiring more energy measurements than comparator channels may incur an additional noise penalty due to decreased dose utilisation. For example, consider a detector with *N* channels that acquire *N* one-sided energy measurements simultaneously. For comparison, consider a detector with one energy channel that acquires *N* energy measurements by sweeping a single threshold across *N* acquisitions. The dose would increase by a factor of *N* if the mean number of detected counts in each bin is required to be

Physics in Medicine and Biology, Vol 60, No. 4 (February 2015): pg. 1583-1600. DOI.

the same as the simultaneous acquisition of the *N* energy-measurements, assuming there are no changes to the spectrum filtration. If the dose is required to be constant, the number of photons acquired by the sequential acquisitions would be a factor of *N* lower than the simultaneous acquisition with *N* comparators, resulting in a $\sqrt{N}$increase in noise standard deviation. A similar noise penalty is incurred in a chess-board detector, where the noise standard deviation increases by a factor equal to the square root of the number sub-pixels set to different energy thresholds.

In summary, when the number of acquired one-sided energy measurements is greater than the number of comparator channels, a subset of the one-sided energy measurements are statistically independent. Two-sided energy bins calculated from independent one-sided energy measurements have increased noise variance and follow a different probability distribution compared to energy bins created by subtracting positively correlated one-sided measurements. Acquiring independent one-sided energy measurements may also incur an additional penalty in dose efficiency. Despite these noise penalties, acquiring more energy measurements than comparator channels has been proposed to potentially increase spectral information (Kappler *et al* 2013) and may be used to simulate detectors with more comparator channels.

2.2. Experimental quantification of noise properties

Experiments were performed to verify the theoretical noise properties discussed in section 2.1 and to quantify the effects of these noise properties on material decomposition and energy weighting images. In this experimental study, the effects of acquiring independent energy measurements were quantified by comparing the noise properties of two positively correlated one-sided energy measurements acquired simultaneously from two channels and the same energy measurements acquired independently by sequential acquisition of a single channel. For these experiments, the additional independent energy measurements were acquired at the same view angle and sub-pixel, but at a different time, which is a general model that can be used to quantify the noise consequences of acquiring more energy measurements than comparator channels. If acquiring more

Physics in Medicine and Biology, Vol 60, No. 4 (February 2015): pg. 1583-1600. DOI.

energy measurements than comparator channels is found to be advantageous in this study, future work could investigate the consequences of acquiring the additional measurements across view angle or sub pixel.

The thresholds were empirically selected at 25 keV and 50 keV and were not optimised for any specific task. In one set of experiments, the dose was doubled when acquiring the energy measurements through sequential acquisition of one channel, so that the measurements contained the same mean number of counts as the simultaneous acquisition from two channels. In this set of experiments, changes in noise were due only to differences in noise correlations across energy measurements. A second set of experiments acquired the two energy measurements sequentially from one channel with the dose equal to the simultaneous, two-channel acquisition. For all acquisitions, two-sided energy bins ([25–50], [50–100] keV) were formed by subtracting the higher threshold measurement from the lower threshold measurements.

Experimental data were acquired on a bench-top spectral CT system shown in figure 1. The bench-top system consists of a CdZnTe detector (NEXIS, Nova R and D, Riverside, CA) with two pixel rows, each consisting of 128, 1 mm pixels and a maximum of five energy thresholds per pixel. The system also contains a microfocal x-ray source (Fein-Focus-100.50, YXLON Intl, Hamburg, Germany) with a 3 micron effective focal spot. Acquisitions were performed at 100 kV and with raw-beam flux of 3×10^5 counts/(s $\cdot$mm^2) compared to a maximum count rate of 2×10^6 counts/(s $\cdot$mm^2). CT images were acquired with a 41 cm source-to-isocenter distance and 72 cm source-to-detector distance. CT images were reconstructed using filtered backprojection onto 0.25 mm × 0.25 mm pixels.

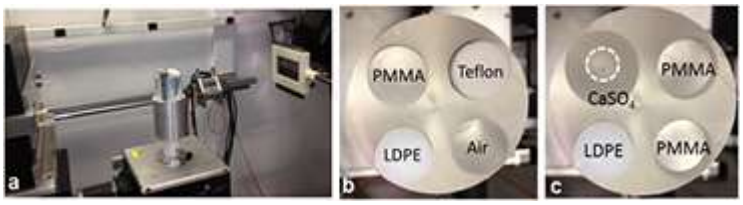

Figure 1. (*a*) Experimental bench-top system, (*b*) phantom used for material decomposition study and (*c*) phantom used for energy-weighting study.

Physics in Medicine and Biology, Vol 60, No. 4 (February 2015): pg. 1583-1600. DOI.

2.2.1. Noise covariance between energy measurements.

The covariance matrix of the acquired one-sided energy measurements was calculated from 1000 measurements through air. Data were acquired at 40 μA and 110 ms per trial for data acquired by simultaneous acquisition of two channels. The acquisition time was doubled to 220 ms per trial when the the two energy measurements were acquired sequentially using one channel, so that the mean number of counts per energy measurement was held constant. Let $\mathbf{X} = [\mathbf{x}_1, ..., \mathbf{x}_B]$ be a K by B matrix, where K is the number of trials (K = 1000) and B is the number of energy measurements (B = 2). The columns of $\mathbf{X}$, $\mathbf{x}_b$, contain K measurements of the number of photons counted above the bth threshold. The covariance matrix for one-sided energy measurements was calculated as:

$$\mathbf{C}_{i,j} = \frac{1}{K-1}\sum_{k=1}^{K}\left(\mathbf{X}_{k,i} - \bar{\mathbf{x}}_i\right)\left(\mathbf{X}_{k,j} - \bar{\mathbf{x}}_j\right) \quad (3)$$

where $\bar{\mathbf{x}}_b$is the mean counts detected above the bth threshold, averaged across the K trials. Because two energy measurements were considered in this experiment, $\mathbf{C}_{i,j}$ was a 2 × 2 matrix.

For each trial, two-sided energy bins were calculated by subtracting the high threshold measurement from the low threshold measurement, forming a matrix $\mathbf{Y} = [\mathbf{y}_1, ..., \mathbf{y}_B]$, as described in equation (4).

$$\begin{aligned}\mathbf{y}_b &= \mathbf{x}_b - \mathbf{x}_{b+1}, b = 1, ..., B-1 \\ \mathbf{y}_B &= \mathbf{x}_B\end{aligned} \quad (4)$$

The covariance matrix for the two-sided energy bins was calculated as:

$$\mathbf{D}_{i,j} = \frac{1}{K-1}\sum_{k=1}^{K}\left(\mathbf{Y}_{k,i} - \bar{\mathbf{y}}_i\right)\left(\mathbf{Y}_{k,j} - \bar{\mathbf{y}}_j\right) \quad (5)$$

2.3. Two-material decomposition

Physics in Medicine and Biology, Vol 60, No. 4 (February 2015): pg. 1583-1600. DOI.

Spectral information can be used to decompose the attenuation coefficient of a material into a linear combination of two or more basis attenuation functions, $f_j(E)$, as expressed in equation (6), where M is the number of basis functions (Alvarez and Macovski 1976). Typical basis functions are the attenuation functions of two basis materials, or functions representing the energy dependence of Compton and photoelectric attenuation. If more than two spectral measurements are acquired, additional basis materials can be decomposed representing the contribution of materials with K-absorption edges in the spectrum range (Roessl and Proksa 2007). The set of basis coefficients, c_j, form a unique material signature.

$$\mu(E) = \sum_{j=1}^{M} c_j f_j(E) \tag{6}$$

The pathlengths through the basis coefficient distributions, $c_j(x, y)$, along ray $\vec{t}$ can be represented with a vector **A**, whose elements A_j are equal to:

$$A_j = \int c_j(x, y)\, \mathrm{d}\vec{t} \tag{7}$$

Substituting equations (6) and (7) into equation (1) forms a system of equations relating the mean number of counts detected in each energy measurement, $\bar{\lambda}_i$, to the the pathlengths through each basis coefficient distribution, **A**.

$$\bar{\lambda}_i = \int_{E_i}^{E_{i+1}} S(E) \exp^{-\sum_{j=1}^{M} A_j f_j(E)} \mathrm{d}E \tag{8}$$

Material decomposition involves estimating the basis material pathlengths, **A** from the number of counts detected in each energy measurement, m_i (Alvarez and Macovski 1976, Roessl and Proksa 2007, Schlomka *et al* 2008). Images of the basis coefficient distribution $c_j(x, y)$, can be reconstructed from sinograms of the estimated basis pathlengths **A** using conventional reconstruction techniques such as filtered backprojection.

Physics in Medicine and Biology, Vol 60, No. 4 (February 2015): pg. 1583-1600. DOI.

In the experimental study, spectral CT data were decomposed into thicknesses of PMMA and aluminium basis materials using the empirical 'A-table' method proposed by Alvarez (2011). In the 'A-table' method, the number of counts detected in the *i*th energy bin, m_i is log-normalised, forming the vector **L**, with elements ℓ_i equal to:

$$\ell_i = -\ln\left(\frac{m_i}{\int_{E_i}^{E_{i+1}} S(E)\,\mathrm{d}E}\right) \tag{9}$$

The A-table method approximates the relationship between the log-normalised measurements **L** and the basis material thicknesses **A**, as expressed in equation (10), where the matrix **M** is estimated through a calibration procedure. The calibration procedure also generates a look up table to correct for the errors in the linear approximation of equation (10).

$$\mathbf{L}(\mathbf{A}) \approx \mathbf{MA} \tag{10}$$

Once the calibration is completed, material decomposition is performed using equation (11), to estimate the unknown basis material thicknesses $\widehat{\mathbf{A}}$from the negative logarithm of spectral transmission measurements **L**, using an estimate of the noise covariance of the data $\mathbf{R}_{L|A}$. $\widehat{\mathbf{A}}$is then adjusted using the correction look up tables created during calibration.

$$\widehat{\mathbf{A}} = \left(\mathbf{M}^T\mathbf{R}_{L|A}^{-1}\mathbf{M}\right)^{-1}\mathbf{M}^T\mathbf{R}_{L|A}^{-1}\mathbf{L} \tag{11}$$

In this work, the calibration data consisted of 25 transmission measurements through all combinations of PMMA (0–4 slabs of 2.54 cm thickness) and aluminium (0–4 slabs of 0.635 cm thickness). Transmission measurements were performed at 0.44 mAs. For each acquisition method investigated in this work, the covariance matrix $\mathbf{R}_{L|A}$ was estimated from the calibration data at the centre of the calibration grid. Therefore, the decomposition algorithm accounted for the noise covariance differences between the studied acquisition methods.

Physics in Medicine and Biology, Vol 60, No. 4 (February 2015): pg. 1583-1600. DOI.

In this study, the effects of acquiring more energy measurements than comparator channels was investigated by performing a CT acquisition of a 6.35 cm-diameter PMMA phantom with 19 mm-diameter inserts of low-density polyethylene, Teflon, Air and PMMA, as shown in figure 1(*b*). Two-hundred acquisitions were performed over 360 degrees at 1.76 mAs for the simultaneous acquisition of the two energy measurements using two channels (25 keV and 50 keV thresholds). The CT data was acquired at 1.76 mAs and 2 × 1.76 mAs when the two energy measurements were acquired sequentially using one channel. Two trials were performed for each acquisition method. The spectral data were decomposed into PMMA and aluminium basis sinograms and reconstructed into basis images. To prevent ring artifacts (caused by spectral inconsistencies across pixels) from affecting the calculation of noise standard deviation, the reconstructed images from the two trials were subtracted to create noise-only images. Noise standard deviation was calculated in 40 × 40 pixel ROIs in the Teflon regions of the noise-only images and divided by the $\sqrt{2}$ to correct for the increased noise due to subtracting two trials.

2.4. Energy-weighted images

One potential advantage of spectral CT acquisition is increased CNR in conventional (non-decomposed) CT images by optimal weighting of the energy data based on its information content (Tapiovaara and Wagner 1985, Shikhaliev 2008). This study investigated the effects of acquiring more energy measurements than comparator channels on optimal energy-weighted images. This study applied optimal image-based weighting, where the final image is a linear combination of the reconstructed energy-bin images (Schmidt 2009). Previous work determined that weighting each energy-bin image proportionally to its contrast-to-noise-variance ratio maximised the CNR in the final image (Schmidt 2009).

Projection images were acquired at 200 angles over 360 degrees, using thresholds of 25 keV and 50 keV, at the same mAs as the material decomposition study. The phantom, displayed in figure 1(*c*), was a 6.35 cm-diameter PMMA cylinder with a 10 mm-diameter $CaSO_4$ cylindrical contrast element. Sinograms of two-sided energy-bin

Physics in Medicine and Biology, Vol 60, No. 4 (February 2015): pg. 1583-1600. DOI.

data were reconstructed into energy bin images. Each acquisition was repeated for two trials.

An estimate of contrast and noise variance is required to calculate the optimal weight for each energy-bin image. ROIs of 40 × 40 pixels were extracted from the contrast element and background regions. Both ROIs were equidistant from the centre of the image. Contrast was estimated in each reconstructed energy-bin image as the difference between the mean value in the calcium ROI and the mean value in the background ROI. In order to prevent ring artifacts from influencing the noise variance estimate, two trials were performed of each acquisition and the resulting reconstructed images subtracted to create images containing only noise. The noise variance in each energy-bin image was estimated as the variance in the background ROI divided by two, where the factor of two accounts for the increased noise due to subtraction of the two image trials.

The optimal image-based weights for each acquisition method and each energy-bin image were calculated as the contrast-to-noise-variance ratio, normalised so that the sum of the weights across energy bins equaled one. For each acquisition method, the energy-bin images were weighted by the corresponding weights and then summed to form the final energy-weighted images. The calcium and background ROIs were extracted from the energy-weighted images to calculate the CNR. For comparison, the CNR was also calculated in an image reconstructed from the number of photons detected above the lowest threshold, resulting in a photon-counting image without spectral information.

2.5. Is There a net benefit when acquiring more measurements than comparator channels?

An analytical and simulation study was performed to investigate whether the additional spectral information obtained by acquiring more energy measurements than comparator channels outweighs the noise penalty of acquiring independent energy measurements. The study assumed an ideal detector to determine whether there is a benefit under ideal conditions and to be general across detector implementations. Also, the study considered only the effects of noise,

dose and spectral information, without considering other tradeoffs that may be necessary to acquire the additional energy measurements (e.g. increased scan time, increased pixel size, or reduced view sampling). If acquiring more energy measurements than comparator channels is found to have potential benefits in this ideal case, future studies can investigate additional tradeoffs and nonideal effects.

This study considered the case of a detector pixel with two comparator channels, which can acquire two simultaneous, correlated one-sided energy measurements. Additional energy information can be obtained by repeating the two-channel acquisition at different thresholds, resulting in two pairs of energy measurements. The one-sided energy measurements within each pair are correlated and are from the same spectrum noise realisation, however the measurements across pairs are independent and from different spectrum realisations. This study investigated the question of whether acquiring four energy measurements with two comparator channels improved material decomposition noise and energy weighted CNR compared to acquiring two energy measurements using two channels.

The comparison of two versus four energy measurements must be performed at the optimal bin thresholds for each type of acquisition. The optimal thresholds are known to vary according to task (Wang and Pelc 2011) and are expected to vary across the investigated acquisition methods. In this study, the optimal thresholds were determined for each studied task and acquisition method, as described in the following sections. The investigated acquisition methods were then compared using the optimal threshold combinations for each method. This study assumed a 120 kV spectrum, Poisson noise and an ideal photon-counting detector. All investigated methods were compared at the same dose. The acquisition methods were compared at the optimal thresholds with respect to noise in material decomposition estimates and the CNR in energy-weighted images for small (15 cm-diameter) and large (35 cm-diameter) objects.

We represent the comparator threshold values as $T_{j,k}$ where j represents the acquisition number and k represents the comparator channel number. One method compared in this study used the two-channel detector to acquire two simultaneous energy measurements

Physics in Medicine and Biology, Vol 60, No. 4 (February 2015): pg. 1583-1600. DOI.

($T_{1,1}$ and $T_{1,2}$). To find the optimal threshold settings, all possible pairs of thresholds were investigated (at 2 keV threshold increments) with the constraints that $T_{1,1} < 40$ keV, $T_{1,1} < T_{1,2}$. For the second investigated method, two pairs of energy measurements were acquired using two sequential acquisitions of the two-channel detector ([$T_{1,1}$, $T_{1,2}$] and [$T_{2,1}$, $T_{2,2}$]). All possible threshold combinations were investigated with the constraints that $T_{1,1} < 40$ keV, $T_{1,1} < T_{1,2}$ and $T_{2,1} < T_{2,2}$. This wide range of threshold combinations included a few interesting cases. When $T_{1,1} < T_{1,2} < T_{2,1} < T_{2,2}$, the acquisition simulated a four-channel detector, although with half the number of counts per bin at dose equal to simultaneous four-channel acquisition and without the positive correlation across the two pairs of measurements. Another interesting case was when $T_{2,1} = T_{1,1} = 20$ keV, in which there was no dose penalty, because the second acquisition used all of the acquired photons. The four-threshold acquisition was equivalent to the simultaneous two-threshold acquisition when both pairs of thresholds were set to the same values ($T_{1,1} = T_{2,1}$, $T_{1,2} = T_{2,2}$).

Each simultaneous pair of energy measurements was processed by subtracting the higher-energy measurement from the lower-energy measurement. In this study, energy-bin measurements were not subtracted between the two pairs of measurements, so that the same processing method could be applied to all investigated threshold combinations. The resulting four energy-bin measurements represented the energy ranges: [$T_{1,1} < E < T_{1,2}$], [$T_{1,2} < E < E_{max}$], [$T_{2,1} < E < T_{2,2}$], [$T_{2,2} < E < E_{max}$], where E_{max} is the highest energy in the spectrum.

To quantify the benefit of the additional energy measurements without the noise penalty, the performance of a pixel with four comparator channels was also investigated ([$T_{1,1}$, $T_{1,2}$, $T_{1,3}$, $T_{1,4}$]).

2.5.1. Material decomposition.

The acquisition of two versus four energy measurements from a two channel detector was compared with respect to the noise in two material decomposition tasks: (1) decomposing 12 cm water +3 cm Teflon into thickness of PMMA and aluminium and (2) decomposing 32 cm water +3 cm Teflon into thicknesses of PMMA and aluminium.

The Cramer Rao Lower Bound (CRLB) is the lowest possible variance of an unbiased estimator. The CRLB can be calculated analytically from the likelihood functions that relate the measurements (number of detected counts) to the estimated parameters (basis material thicknesses). The CRLB has been used in previous spectral CT studies to compare estimators and to investigate acquisition effects (Roessl *et al* 2007, Roessl and Herrmann 2009, Wang and Pelc 2011). Because each simultaneous pair of energy measurements was processed by subtracting the higher-energy measurement from the lower-energy measurement without subtracting between independent pairs of measurements, the number of counts in the resulting two-sided energy bins were independent and Poisson distributed. Therefore the CRLB expressions determined in previous material decomposition studies could be applied (Roessl and Proksa 2007, Wang and Pelc 2011). In this study, the CRLB variance was calculated at all threshold settings to determine the optimal thresholds. The CRLB variance was then compared at the optimal thresholds for two energy measurements from two channels, four energy measurements from two channels and four energy measurements from four channels.

2.5.2. Energy weighting.

Because of the large number of possible bin combinations, this study developed an approximate analytical method to determine the optimal thresholds that maximised the CNR of an optimally weighted image for a given task. The analytical approximation is presented in appendix A. The investigated objects were: (1) 15 cm-diameter water cylinder with embedded 1 cm-diameter $CaCO_3$ contrast element and (2) 35 cm-diameter water cylinder with 1 cm-diameter $CaCO_3$ element. The analytical method presented in appendix A determined the optimal threshold combinations for each investigated acquisition method. Because the analytical method described in appendix A is approximate, CT simulations were then performed at the optimal thresholds for each investigated object and acquisition method. The optimal weights and resulting CNR were calculated from regions of interest in the reconstructed images, as previously described (Schmidt 2009).

Physics in Medicine and Biology, Vol 60, No. 4 (February 2015): pg. 1583-1600. DOI.

3. Results

3.1. Experimental quantification of noise properties

3.1.1. Variance and covariance between energy measurements.

Table 1 displays the variance in one-sided low and high energy measurements acquired from two simultaneous comparator measurements and from two independent measurements using one comparator. Both acquisition methods resulted in the same variance in one-sided energy measurements, because both were acquired with the same mean number of counts per measurement. Table 1 also displays the covariance between the low and high energy measurements. As predicted in section 2.1, the one-sided energy measurements acquired simultaneously from two channels demonstrate high positive covariance, while the measurements acquired independently demonstrate small covariance (~ 5% of the variance).

Table 1. Comparison of variances in low and high energy measurements acquired by two simultaneous channels and by independent measurements using one channel.

	Two simultaneous channels	Two independent measurements with one channel
Variance in one-sided low-energy measurement ($\mathbf{C}_{1,1}$)	17 959	17 960
Variance in one-sided high-energy measurement ($\mathbf{C}_{2,2}$)	15 894	14 080
Covariance between low and high one-sided energy measurement ($\mathbf{C}_{1,2}$)	15 015	1010
Variance in two-sided low-energy bin ($\mathbf{D}_{1,1}$)	3824	30 019
Variance in two-sided high-energy bin ($\mathbf{D}_{2,2}$)	15 894	14 080
Covariance between low and high two-sided energy bins ($\mathbf{D}_{1,2}$)	−879	−13 070

Note: The covariance between the low and high energy measurements is also displayed. The table also displays the variances and covariance of resulting two-sided energy bins, obtained by subtracting the high-energy one-sided measurement from the one-sided low-energy measurement. Variances and covariances were calculated using equation (3) for one-sided measurements and using equation (5) for two-sided energy bins.

Physics in Medicine and Biology, Vol 60, No. 4 (February 2015): pg. 1583-1600. DOI.

Table 1 also displays the variance in the low and high energy two-sided bins, resulting from subtracting the high energy one-sided measurement from the low-energy one-sided measurement, along with the covariance between the resulting low and high energy bins. Variances and covariances are displayed for measurements acquired using two simultaneous comparator channels and two independent measurements from one comparator. Both investigated acquisition methods resulted in a similar mean number of photons detected in the lowest energy two-sided bin. However, as predicted in section 2.1, acquiring two independent energy measurements using one channel increased the noise variance in the two-sided low-energy bin by a factor of 7.9. Because the second energy bin is a one-sided bin (all photons greater than the highest threshold), the noise depends only the noise in that energy range and is the same for both acquisition methods. The 7.9 factor increase in noise variance for the lower energy bin was due only to the penalty of acquiring independent one-sided energy measurements, as the dose was increased by a factor of two in this experiment to maintain the same mean number of counts per measurement. The variance would increase by an additional factor of 2 in all bins if the dose was held constant when comparing two simultaneous measurements from two channels to two sequential measurements from one channel. The two-sided energy bins acquired from the two simultaneous channels demonstrated negligible covariance, while two-sided energy bins acquired from independent, sequential acquisition of one channel demonstrated negative covariance. When the one-sided energy measurements are independent, if the noise in the higher-energy measurement causes the detected number of counts to be higher than the expected value, then subtracting this count from the low energy measurement will reduce the number of counts in the resulting two-sided energy bin, causing negative covariance.

3.1.2. Two-material decomposition.

Figure 2 compares the reconstructed PMMA and aluminium basis images decomposed from two energy measurements acquired simultaneously by two channels and sequentially by one channel. The noise standard deviation in the Teflon region of the basis images is also presented in figure 2. To isolate the effects of covariance across energy measurements, the acquisition of two energy measurements

Physics in Medicine and Biology, Vol 60, No. 4 (February 2015): pg. 1583-1600. DOI.

using one channel was performed with the dose increased by a factor of two to maintain the same mean number of counts as in the simultaneous acquisition with two channels. Data was also acquired at dose equal to the simultaneous, two-channel acquisition. The covariance penalty from acquiring independent energy measurements increased the noise standard deviation in the reconstructed basis images by factors of 1.5–1.7, with an additional factor of 1.4 noise increase due to decreased dose utilisation. The mean values in the Teflon region varied by less than 1% across all reconstructed basis images, demonstrating that acquiring independent energy measurements affected the noise but not the mean values.

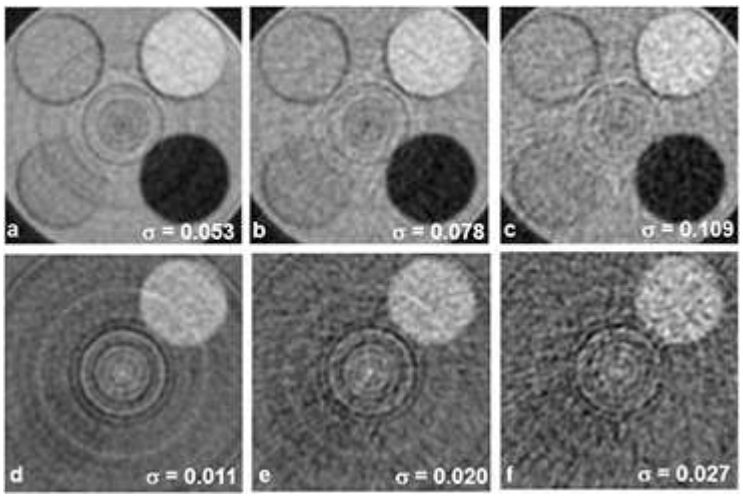

Figure 2. (top) PMMA and (bottom) aluminium basis images reconstructed from two energy measurements displayed at the same window and level for each row. The pixel values represent the PMMA and aluminium basis material coefficients, respectively (c_j's in equation (6)). Images (*a*) and (*d*) were reconstructed from correlated energy measurements acquired simultaneously using two channels. Images (*b*) and (*e*) were reconstructed from independent one-sided energy measurements acquired from sequential acquisitions by one channel with the dose increased by a factor of two to maintain the mean number of counts. Images (*c*) and (*f*) were reconstructed from independent one-sided energy measurements acquired by one channel, at the same dose as images (*a*) and (*d*).

3.1.3. Energy weighting.

To demonstrate the effects of the acquisition methods on the noise in reconstructed energy-bin images, figure 3 displays images reconstructed from the two-sided [25–50] keV energy bin calculated by the subtracting the low/high energy measurements acquired simultaneously from two channels and sequentially from one channel

Physics in Medicine and Biology, Vol 60, No. 4 (February 2015): pg. 1583-1600. DOI.

(at twice the dose and equal dose). All images contained similar contrast levels between the calcium element and background. The change in covariance across energy measurements due to acquiring independent energy measurements increased the noise standard deviation by a factor of 1.7. The reduced dose efficiency of acquiring two sequential scans increased the noise by an additional factor of 1.4. When considering the combined effects of covariance and dose efficiency, acquiring the two energy measurements independently using one channel increased the noise in this energy bin by a factor of 2.4 at dose equal to the simultaneous acquisition using two channels.

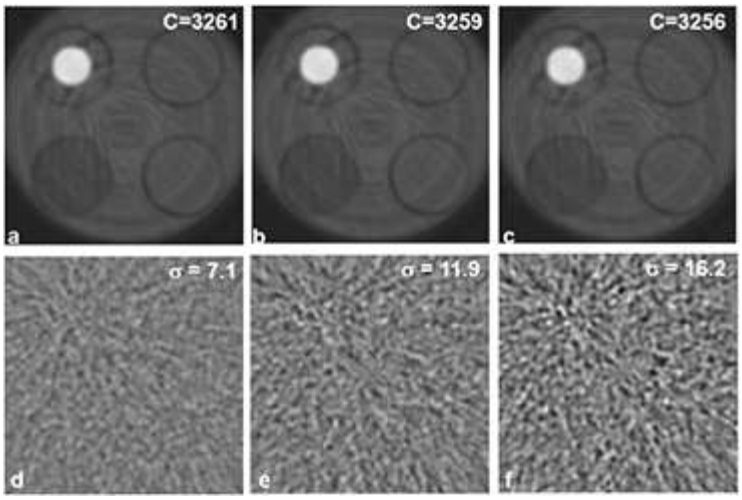

Figure 3. (top) Reconstructed phantom images and (bottom) noise-only images from the [25–50] keV energy bin, displayed at the same window and level for each row. The pixel values represent the reconstructed linear attenuation coefficients in the energy bin. Images (*a*) and (*d*) were derived from two energy measurements acquired simultaneously using two channels. Images (*b*) and (*e*) were derived from two independent energy measurements acquired by sequential scanning using one channel with the mean number of counts held constant, while images (*c*) and (*f*) were derived from independent measurements with the dose held constant.

Figure 4 displays the optimal energy-weighted images reconstructed from two energy measurements acquired simultaneously using two channels and sequentially using one channel. For comparison, the image reconstructed from the number of counts above the lowest energy threshold (i.e. photon counting image) is also displayed. The CNR and noise standard deviation of each acquisition is also displayed in figure 4. The optimal bin weights varied for the investigated methods, yielding optimally weighted images with different contrast levels.

Physics in Medicine and Biology, Vol 60, No. 4 (February 2015): pg. 1583-1600. DOI.

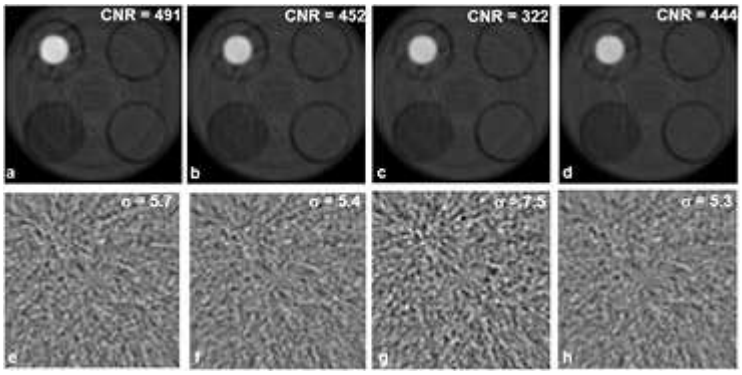

Figure 4. (top) Reconstructed phantom images and (bottom) noise-only images, displayed at the same window and level for each row. The pixel values represent the estimated linear attenuation coefficients, which depend on the optimal weights. Images (*d*) and (*h*) were reconstructed from the photon-counting measurement. All other images are optimally weighted images reconstructed from two energy bins. Images (*a*) and (*e*) were reconstructed from energy measurements acquired simultaneously using two channels. Images (*b*) and (*f*) were reconstructed from energy measurements acquired independently using one channel with the dose increased by a factor of two to maintain the same mean number of counts. Images (*c*) and (*g*) were reconstructed from energy measurements acquired independently using one channel at the same dose as images acquired from simultaneous acquisition using two channels.

The changes in covariance due to acquiring independent energy measurements decreased the CNR by a factor of 0.92, while the reduction in dose utilisation of requiring two scans reduced the CNR by an additional factor of 0.71, resulting in an overall reduction of CNR by a factor of 0.66. Acquiring two simulataneous energy measurements improved the CNR by a factor of 1.1 compared to the photon-counting image resulting from one comparator measurement. However, when the one comparator was used to sequentially acquire two energy measurements, the CNR was reduced by a factor of 0.73 compared to the photon-counting image at equal dose.

3.2. Is there a net benefit when acquiring more measurements than comparator channels?

Table 2 presents the results of the investigation of whether acquiring four energy measurements from two channels had a benefit in material decomposition noise compared to acquiring two energy measurements from two channels. The acquisition of four energy measurements from two channels had the lowest noise variance when the two pairs of simultaneous two-channel acquisitions used the same energy thresholds ($T_{1,1} = T_{2,1}$, $T_{1,2} = T_{2,2}$), resulting in an acquisition

that was equivalent to the two-channel/two-measurement acquisition. These result demonstrate no benefit when acquiring more energy measurements than channels. There was 20–25% noise reduction when acquiring four energy measurements from four simultaneous channels. The results suggest that while there is a benefit of simultaneously acquiring four energy measurements compared to two energy measurements, the noise penalty of acquiring two independent pairs of measurements outweights this benefit.

Table 2. Comparison of noise standard deviation in two-material decomposition estimates obtained by acquisition of two energy measurements from two channels, four energy measurements from two channels and four energy measurements from four channels, as described in section 2.5.

Number of comparator channels	2	2	4
Number of energy measurements	2	4	4
PMMA image noise (15 cm phantom)	0.14	0.14	0.12
Aluminium image noise (15 cm phantom)	0.042	0.042	0.035
Optimal thresholds (15 cm phantom)	[20, 50]	[20, 50], [20, 50]	[20, 40, 50, 68]
PMMA image noise (35 cm phantom)	1.43	1.43	1.16
Aluminium image noise (35 cm phantom)	0.48	0.48	0.39
Optimal thresholds (35 cm phantom)	[20, 66]	[20, 66], [20, 66]	[20, 48, 58, 74]

Note: The noise standard deviation in PMMA and aluminium basis images are displayed, along with the optimal thresholds for each acquisition type. The last column contains four optimal thresholds for the four channel acquisition.

Table 3 presents the results of the investigation of whether acquiring four energy measurements from two channels had a benefit in the CNR of optimal energy weighted images. As in the case of material decomposition, the results demonstrated no benefit when acquiring more energy measurements than channels, with the optimal thresholds for the two channel/four measurement acquisition equal to the two-channel/two-measurement acquisition. Acquiring four energy measurements from four simultaneous channels increased the CNR by 5%.

Table 3. Comparison of CNR in optimal energy weighted images from acquisition of two energy measurements from two channels, four energy measurements from two channels and four energy measurements from four channels, as described in section 2.5.

Number of comparator channels	2	2	4
Number of energy measurements	2	4	4
CNR (15 cm phantom)	46.4	46.4	47.8
Optimal thresholds (15 cm phantom)	[28, 50]	[28, 50], [28, 50]	[26, 40, 50, 70]
CNR (35-cm phantom)	4.6	4.6	4.7
Optimal thresholds (35 cm phantom)	[38, 66]	[38, 66], [38, 66]	[34, 48, 58, 76]

Physics in Medicine and Biology, Vol 60, No. 4 (February 2015): pg. 1583-1600. DOI.

Note: the CNR values are displayed, along with the optimal thresholds for each acquisition type. The last column contains four optimal thresholds for the four comparator acquisition.

4. Discussion

The experimental study demonstrated increased noise when acquiring more energy measurements than comparator channels, as predicted in the theoretical discussion (section 2.1). The experimental study then demonstrated how the increased noise and different noise covariances propagated into material decomposition estimates and energy weighted images. In the experimental study, the effects of noise covariance resulted in a factor of 1.5–1.7 noise standard deviation increase in decomposed basis images and a factor of 0.92–0.71 reduction in CNR in energy-weighted images. Noise standard deviation increased by an additional factor of $\sqrt{2}$ due to reduced dose utilisation and in general would increase by a factor of $\sqrt{N}$, where N is the number of additional measurements required to collect the spectral data.

The analytical study of optimal detector configurations determined that acquiring four energy measurements from four simultaneous channel measurements reduced noise and increased CNR compared to acquiring two energy measurements from two simultaneous channels. However, there was no benefit in noise or CNR when the four energy measurements were acquired using two sequential acquisitions by a two-channel detector, due to the noise penalty of acquiring independent energy measurements. When acquiring four energy measurements using a two-channel detector, the optimal thresholds resulted in the effective acquisition of two energy measurements.

The analytical study assumed an ideal photon-counting detector. In practice, the energy resolution of photon-counting detectors is limited by numerous non-ideal effects such as pulse-pileup, charge sharing, k-escape and other effects (Schlomka *et al* 2008, Taguchi *et al* 2010, Cammin *et al* 2014). Since the study determined no benefit when acquiring more energy measurements than comparator channels for a detector with ideal energy resolution, it is expected that the same conclusion would be true for realistic detectors with degraded energy

Physics in Medicine and Biology, Vol 60, No. 4 (February 2015): pg. 1583-1600. DOI.

resolution, as the additional energy measurements would contain less information than in the ideal detector.

This study investigated two-material decomposition. Three-material decomposition to isolate the contributions of a K-edge material requires at least three energy measurements (Roessl and Proksa 2007). For K-edge imaging, acquiring a third independent energy measurement may be beneficial compared to a simultaneous two-channel acquisition or a single channel acquisition, although this requires additional investigation. The results of this study indicate that three-material decomposition would have the lowest noise when acquired simultaneously by three comparator channels from the same spectrum noise realisation.

The results suggest no benefit when acquiring more energy measurements than channels. However, this mode of operation may be required for prototype detectors with a limited number of channels to simulate or investigate feasibility of a detector with more channels. The results of this study suggest the following implications when using a detector with a limited number of comparator channels to simulate a detector with more channels.

- A detector with one comparator channel cannot accurately simulate a detector with multiple comparator channels. If the single comparator threshold is swept to acquire additional energy measurements, the independent one-sided energy measurements and resulting two-sided energy-bin measurements contain increased noise and different noise statistics than a multiple channel detector. Bias can be introduced if incorrect noise statistics are assumed in the material decomposition algorithm (Yavuz and Fessler 1999).
- A detector with two comparator channels can simulate a detector with multiple comparator channels if a two-channel acquisition is performed to acquire each two-sided energy bin. This acquisition would result in the same noise and noise statistics as a detector with more detector channels, although the dose would increase proportionally to the total number of two-sided energy bins. The increased dose may be acceptable for phantom experiments.

Physics in Medicine and Biology, Vol 60, No. 4 (February 2015): pg. 1583-1600. DOI.

5. Conclusions

Spectral CT projection data is usually derived from correlated one-sided energy measurements acquired simultaneously using a dedicated comparator channel for each energy measurement. Due to readout electronics complexity, some spectral CT designs form two-sided energy bins from independent one-sided energy measurements, by acquiring more energy measurements than comparator channels. The results demonstrated that this method increased noise variance, or equivalently patient dose. Furthermore, this noise amplification is expected to increase with the number of independent energy measurements. The results suggest that there is no benefit in two-material decomposition noise or energy-weighted CNR when acquiring more energy measurements than comparator channels. Understanding the noise penalty of acquiring more energy measurements than comparator channels is important for designing spectral detectors and for designing experiments and interpreting data from prototype systems with a limited number of comparator channels.

Acknowledgments

This work was supported by NIH Grant number R21EB015094. The contents of this article are solely the responsibility of the authors and do not necessarily represent the official views of the National Institutes of Health. The authors acknowledge S Haworth, Medical College of Wisconsin, for assistance with the experimental system.

Appendix A: Analytical approximation of optimal energy weighted CNR

An expression for the optimal CNR resulting from image-based weighting, CNR_{IW}, was derived in a previous study (Schmidt 2009). For investigating the net benefit of acquiring more energy measurements than thresholds, (section 2.1), an analytical method was required to determine the optimal bin thresholds that maximise CNR_{IW}. This analytical method requires an estimate of the contrast and noise in each energy bin. Estimating the contrast requires an estimation of the attenuation coefficients in the background and contrast element regions of the *i*th energy bin, $\widehat{\mu}_{\text{water},i}$ and $\widehat{\mu}_{\text{calc},i}$, respectively.

In this study, $\hat{\mu}_{\text{water},i}$ and $\hat{\mu}_{\text{calc},i}$ were calculated as the attenuation coefficients that would be obtained using transmission measurements through known thicknesses of materials representing the central ray through the cylinder. The mean number of counts detected in the *i*th energy bin, $\bar{\lambda}_i$, for the central ray through the cylinder, is expressed in equation (A.1), where x_{water} and x_{calc} are the thicknesses of water and calcification along the diameter of the cylinder.

$$\bar{\lambda}_i = \int_{E_i}^{E_{i+1}} S(E)\, \mathrm{e}^{-\left(\mu_{\text{water}}(E)x_{\text{water}} + \mu_{\text{calc}}(E)x_{\text{calc}}\right)} \qquad \text{(A.1)}$$

The water and calcification attenuation coefficients were approximated using:

$$\hat{\mu}_{\text{water},i} = -\ln\left(\frac{\bar{\lambda}_i}{\int_{E_i}^{E_{i+1}} S(E)\, \mathrm{e}^{-\left(\mu_{\text{calc}}(E)x_{\text{calc}}\right)}}\right)\cdot\frac{1}{x_{\text{water}}} \qquad \text{(A.2)}$$

$$\hat{\mu}_{\text{calc},i} = -\ln\left(\frac{\bar{\lambda}_i}{\int_{E_i}^{E_{i+1}} S(E)\, \mathrm{e}^{-\left(\mu_{\text{water}}(E)x_{\text{water}}\right)}}\right)\cdot\frac{1}{x_{\text{calc}}} \qquad \text{(A.3)}$$

The noise variance in each energy-bin image was approximated as the inverse of the mean number of counts detected in each bin for the central ray through the phantom, $\bar{\lambda}_i$ (Chesler *et al* 1977). The noise variances approximated using this method were proportional to the true noise variance, which was sufficient for calculating the optimal weights, because the optimal weights were normalised to have a sum of one.

The approximate CNR_{IW} was calculated for all studied threshold combinations. The optimal thresholds were selected as the threshold combination that maximised CNR_{IW}.

To validate that the approximate analytical method was adequate for optimising the bin thresholds, the optimal thresholds for the two-threshold acquisition were determined using the analytical approximation and using simulated CT data for the 15 cm phantom. To reduce the simulation load, the lower threshold was set to 20 keV for this validation study. In the simulations, the optimal weights and CNR_{IW} were calculated using estimates of contrast

Physics in Medicine and Biology, Vol 60, No. 4 (February 2015): pg. 1583-1600. DOI.

and noise variance from regions in the reconstructed images. Figure 5 plots the CNR_{IW} estimated using the analytical approximation and through simulations for varying values of the higher energy threshold. Both CNR curves were normalised by their mean, because the analytical noise approximation is only proportional to the true noise variance. Figure 5 demonstrates that the analytical method was able to identify the threshold setting with the highest CNR. As described in section 2.5.2, simulations were performed at these optimal threshold settings to compare the CNR between the different acquisition methods.

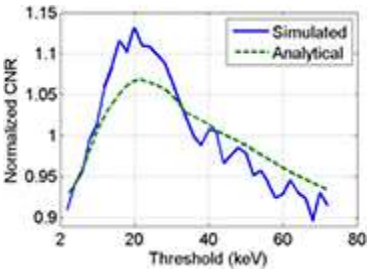

Figure 5. The optimal energy weighting CNR, CNR_{IW}, as estimated using the analytical approximation and through simulations for a range of high-energy threshold values. The CNR values for each method were normalised by the mean value across thresholds.

References

Alvarez R 2011 Estimator for photon counting energy selective x-ray imaging with multibin pulse height analysis Med. Phys. ***38*** *2324*

Alvarez R E and Macovski A 1976 Energy-selective reconstructions in x-ray computerised tomography *Phys. Med. Biol.* **21** 733–44

Cammin J, Xu J, Barber W C, Iwanczyk J S, Hartsough N E and Taguchi K 2014 A cascaded model of spectral distortions due to spectral response effects and pulse pileup effects in a photon-counting x-ray detector for CT *Med. Phys.* **41** 041905

Chesler D A, Riederer S J and Pelc N J 1977 Noise due to photon counting statistics in computed x-ray tomography *J. Comput. Assist. Tomogr.* **1** 64–74

Kappler S, Henning A, Krauss B, Schoeck F, Stierstorfer K, Weidinger T and Flohr T 2013 Multi-energy performance of a research prototype CT scanner with small-pixel counting detector *Proc. SPIE* **8668** 86680O

Procz S, Lubke J, Zwerger A, Mix M and Fiederle M 2009 Optimization of medipix-2 threshold masks for spectroscopic x-ray imaging *IEEE Trans. Nucl. Sci.* **56** 1795–9

Roessl E and Herrmann C 2009 Cramér–Rao lower bound of basis image noise in multiple-energy x-ray imaging *Phys. Med. Biol.* **54** 1307

Physics in Medicine and Biology, Vol 60, No. 4 (February 2015): pg. 1583-1600. DOI.

Roessl E and Proksa R 2007 K-edge imaging in x-ray computed tomography using multi-bin photon counting detectors *Phys. Med. Biol.* **52** 4679–96

Roessl E, Ziegler A and Proksa R 2007 On the influence of noise correlations in measurement data on basis image noise in dual-energylike x-ray imaging *Med. Phys.* **34** 959–66

Schlomka J P et al 2008 Experimental feasibility of multi-energy photon-counting K-edge imaging in pre-clinical computed tomography *Phys. Med. Biol.* **53** 4031–47

Schmidt T G 2009 Optimal 'image-based' weighting for energy-resolved CT *Med. Phys.* **36** 3018–27

Shikhaliev P M 2008 Computed tomography with energy-resolved detection: a feasibility study *Phys. Med. Biol.* **53** 1475–95

Shikhaliev P M, Xu T and Molloi S 2005 Photon counting computed tomography: concept and initial results *Med. Phys.* **32** 427–36

Taguchi K, Frey E, Wang X, Iwanczyk J and Barber W 2010 An analytical model of the effects of pulse pileup on the energy spectrum recorded by energy resolved photon counting x-ray detectors *Med. Phys.* **37** 3957

Taguchi K and Iwanczyk J S 2013 Vision 20/20: single photon counting x-ray detectors in medical imaging *Med. Phys.* **40** 100901

Tapiovaara M J and Wagner R F 1985 SNR and DQE analysis of broad spectrum x-ray imaging *Phys. Med. Biol.* **30** 519–29

Wang A S and Pelc N J 2011 Sufficient statistics as a generalization of binning in spectral x-ray imaging *IEEE Trans. Med. Imaging* **30** 84–93

Yavuz M and Fessler J A 1999 Penalized-likelihood estimators and noise analysis for randoms-precorrected PET transmission scans *IEEE Trans. Med. Imaging* **18** 665–74

Citations

[1]Spectrum reconstruction method based on the detector response model calibrated by x-ray fluorescence Ruizhe Li et al 2017 *Physics in Medicine and Biology* **62** 1032

[2]Pulmonary CT and MRI phenotypes that help explain chronic pulmonary obstruction disease pathophysiology and outcomes Eric A. Hoffman et al 2016 *Journal of Magnetic Resonance Imaging* **43** 544

[3]Evaluation of conventional imaging performance in a research whole-body CT system with a photon-counting detector array Zhicong Yu et al 2016 *Physics in Medicine and Biology* **61** 1572

[4]Spectral prior image constrained compressed sensing (spectral PICCS) for photon-counting computed tomography Zhicong Yu et al 2016 *Physics in Medicine and Biology* **61** 6707

[5]A neural network-based method for spectral distortion correction in photon counting x-ray CT Mengheng Touch et al 2016 *Physics in Medicine and Biology* **61** 6132